Chemosphere 308 (2022) 136541

Contents lists available at ScienceDirect

Chemosphere

journal homepage: www.elsevier.com/locate/chemosphere

Effects of NO_2 and RH on secondary organic aerosol formation and light absorption from OH oxidation of *o*-xylene

Shijie Liu [a,b], Yiqian Wang [a], Xinbei Xu [a], Gehui Wang [a,b,*]

[a] Key Lab of Geographic Information Science of the Ministry of Education, School of Geographic Sciences, East China Normal University, Shanghai, 210062, China
[b] Institute of Eco-Chongming, 3663 North Zhongshan Road, Shanghai, 200062, China

HIGHLIGHTS

- A chamber study of the compound effect of NO_2 and RH on the *o*-xylene SOA formation through OH-oxidation.
- The evolution characteristics of the *o*-xylene SOA chemical compositions were studied by the HR-ToF-AMS.
- The *o*-xylene SOA mass concentration increased with initial NO_2 concentration at dry condition, but decreased at high RH condition.
- Both the increasing NO_2 concentration and RH condition is beneficial to increase the MAC value of *o*-xylene-derived SOA.

GRAPHICAL ABSTRACT

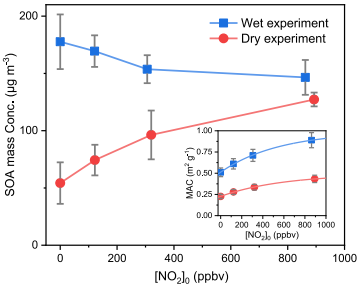

ARTICLE INFO

Handling Editor: Volker Matthias

Keywords:
o-xylene
Secondary organic aerosol
Nitrogen dioxide
Mass absorption coefficient
Aerosol mass spectrometry

ABSTRACT

O-xylene is an important aromatic volatile organic compound (VOC) in the atmosphere over urban areas. In this work, the effect of nitrogen dioxide (NO_2) concentration and relative humidity (RH) on the mass concentration of secondary organic aerosols (SOA) formed from *o*-xylene OH oxidization was investigated in a photooxidation chamber. The *o*-xylene SOA mass concentration increased from 54.2 μg m^{-3} to 127.2 μg m^{-3} during dry conditions, but decreased from 177.7 μg m^{-3} to 146.5 μg m^{-3} during high RH conditions when the initial NO_2 concentration increased form 0 ppbv to about 900 ppbv. An increase in the ratio of $[NO_3^-]/[Org]$ and a decrease in the oxidation state of carbon (OS_C) of SOA suggested that acid-catalyzed heterogeneous reaction was responsible for enhancing SOA formation with increasing NO_2 concentrations in dry conditions. In contrast, in humid conditions, the high molecular diffusion capacity of SOA could promote the reactivity of OH towards the interior of SOA, and the enhancement of nitrous acid (HONO) formation under high NO_2 conditions could promote the SOA aging processes and be responsible for the decreasing trend of SOA formation with NO_2. Light absorption by SOA was also measured, and both NO_2 and RH enhanced the mass absorption coefficient ($MAC_{\lambda = 365\ nm}$) value for the optical properties of *o*-xylene SOA. The highest $MAC_{\lambda = 365\ nm}$ value of *o*-xylene SOA was 0.89 $m^2\ g^{-1}$, observed during humid conditions with an initial NO_2 concentration of 862 ppbv, which was 3.9 times higher than in the experiment conducted in the absence of NO_2 under dry conditions. The formation of nitrogen-containing organic compounds (NOCs) and humic-like substances (HULIS) were responsible for the increased $MAC_{\lambda = 365\ nm}$ values of *o*-xylene derived SOA. This study provides new insight into the effect of NO_2 on

* Corresponding author. Key Lab of Geographic Information Science of the Ministry of Education, School of Geographic Sciences, East China Normal University, Shanghai, 210062, China.
E-mail address: ghwang@geo.ecnu.edu.cn (G. Wang).

https://doi.org/10.1016/j.chemosphere.2022.136541
Received 11 July 2022; Received in revised form 13 September 2022; Accepted 16 September 2022
Available online 20 September 2022

SOA formation through the change in *o*-xylene photooxidation under different RH conditions, and the complex effect of multiple environmental factors on SOA formation was also important and should not be ignored.

1. Introduction

Secondary organic aerosols (SOA) are an important component of atmospheric aerosols and have adverse effects on ambient air quality and human health (George et al., 2015; Gu et al., 2021). The class of organic aerosol called brown carbon (BrC), which exhibits exponentially increasing absorption in the light spectrum from the visible to ultraviolet (UV) wavelength, could also affect the solar radiation balance and even regional climates (Noziere et al., 2015; Zhang et al., 2017; Liu et al., 2021c). The importance of SOA in the atmospheric environment has been widely recognized. However, due to the diversity of SOA precursors, reaction pathways, and environment impact factors (Liu et al., 2021b; Gaubert et al., 2021; Aruffo et al., 2022), the mechanism of SOA formation are still not clear, and attempts at large-scale atmospheric simulations have not achieved good agreement with SOA concentrations from field observations (Charan et al., 2019; Huang et al., 2020; Gaubert et al., 2021).

Nitrogen oxides ($NO_x = NO + NO_2$) are not only the predominant gaseous pollutant in the atmosphere, but also the most important driver of atmospheric oxidation reactions (Zhang et al., 2015). The photolysis of NO_x at different levels has been closely linked to the formation and concentrations of main atmospheric oxidants (such as OH and O_3) in the atmosphere, which participate in the initial oxidation steps of SOA formation (Li et al., 2022). The fate of peroxy radical (RO2) intermediates produced by photooxidation of volatile organic compounds (VOCs) was also linked to NO_x levels (Sarrafzadeh et al., 2016; Zhao et al., 2018). With increasing NO_x concentration, RO2 react more with NO, rather than with HO2, and are rapidly converted to the alkoxy radicals (RO), which produces more high volatile compounds through fragmentation to suppress SOA formation. However, NO_x has also been widely reported to promote SOA formation. In recent years, highly oxygenated organic molecules (HOMs) derived from RO2 autoxidation have been considered another key to SOA formation processes. An alkyl radical (R·) with hydroperoxide functionality will form through hydrogen (H)-shift isomerization reactions from RO2 in the presence of NO. New RO2 will be formed by adding O2 to R·. HOMs with low-volatility compounds would then be formed through repetition of the autoxidation process and promote SOA formation in the presence of NO_x (Bianchi et al., 2019; Li et al., 2022). Nitrogen-containing organic compounds (NOCs) could also be formed through the RO2 + NO reaction, and the effects of NOCs on the nucleation, concentrations, and physicochemical properties of SOA should not be ignored (Ng et al., 2007a; Xu et al., 2015). Liu et al. (2021c) pointed out that the mass concentration ratio of nitrate ions to SOA increased with increasing initial NO_2 concentration, which suggested that the acid-catalyzed reaction would be enhanced by an increase in the NO_2 concentration, which might another important mechanism underlying the promotion effect of NO_2 on SOA formation (Liu et al., 2021c).

Although the effect of NO_2 on SOA formation has been widely reported in previous experimental studies, the combined impacts of NO_2 and other environmental factors on the formation of SOA have not received sufficient attention. Liu et al. (2021b) reported that more semi-volatile oxidation products were formed at higher NO_2 concentrations, and they inhibited SOA yield. However, the presence of NH_3 increased the distribution efficiency of semi-volatile oxidation products in the particle phase, resulting in an increased SOA yield. When SO_2 was present, it was converted to sulfuric acid, which promoted SOA formation by increasing aerosol acidity (Jang et al., 2002; Chu et al., 2016). In the photooxidation process, sulfate formation was enhanced at high NO_2 concentrations, and some studies have pointed out that this enhancement of SOA yield due to particle acidity was only observed in high-NO_2 conditions rather than in low-NO_2 conditions (Offenberg et al., 2009; Eddingsaas et al., 2012; Wang et al., 2016a; Liu et al., 2019a). The role of water in SOA formation has also been inconsistent among studies. Jia and Xu (2018) pointed out that the oligomerization reaction of stable Criegee intermediates (SCIs) from the O_3 channel was obstructed at high relative humidity (RH), which enhanced SOA formation, but the opposite effect of RH was observed on SOA formation in the OH-oxidation channel. The different relative proportions of O_3- and OH-oxidation channels with different NO_2 concentrations in the VOC photooxidation process might be a key factor underlying the inconsistencies in the effect of RH on SOA formation. Above all, the effect of NO_2 on SOA formation with the change in other environmental factors is complex and should be clarified to further understand the mechanisms of SOA formation.

In the atmosphere of urban areas, aromatic compounds are the main VOCs, and they often dominate SOA formation (Zhang et al., 2019b; Gu et al., 2021). Therefore, in the present study, *o*-xylene was used to study the effect of NO_2 on SOA formation under different RH conditions. This paper presents the evolution of SOA mass concentration, optical characteristics, and chemical components of SOA from *o*-xylene under controlled NO_2 and RH conditions. Meanwhile, the relationships between the optical properties and chemical compositions of *o*-xylene derived SOA were also characterized.

2. Experimental methods

2.1. Chamber studies

All experiments were performed in a Teflon photooxidation chamber built in the East China Normal University. The description and characterization results of the chamber have been described in detail in previous studies (Liu et al., 2021b, 2021c), and only a brief introduction is provided here. A 5 m^3 chamber made with the Teflon-FEP film (0.06 mm) was located in a temperature controlled stainless steel cube. UV-light lamps (TUV36W, Philips), which were used to drive OH radical formation through hydrogen peroxide (H_2O_2) photolysis, surrounded the chamber. The light spectrum of UV-light had a peak intensity at 254 nm. Prior to each experiment, the chamber was initially evacuated and then filled with purified air for cleaning. The cycle of filling-purging was performed more than 3 times to reduce the concentrations of residual hydrocarbons, O_3, and NO_2 to less than 1 ppbv, and the concentration of aerosols was less than 10 m^{-3}.

For the photooxidation experiment, the chamber was filled with zero air up to 5 m^3. Zero air was generated using a zero-air supply (111-D3N, Thermo Scientific™, USA), and it was humidified through introduction into a gas-washing bottle filled with high-purity water. The RH of zero air was controlled to create dry (~20% RH) or humid (~70% RH) conditions during different experiments. A known volume of liquid *o*-xylene (Sigma-Aldrich, analytically pure) was first injected into a Teflon FEP tube and then dispensed into the chamber with zero air. In the chamber, *o*-xylene concentrations were calculated were calculated from the injection volume of the liquids. Different volumes of NO_2 (Air Liquid Shanghai, 510 ppm NO_2 in N_2) were introduced into the chamber directly from standard cylinders for the required concentrations. The initial conditions for different experiments are summarized in Table 1. The concentrations of *o*-xylene and NO_2 in the experiments were higher than those in the real atmosphere to keep the particle production significant enough for the off-line collections and accurate measurements. The *o*-xylene concentrations remained stable in the different experimental conditions, the variations of *o*-xylene-derived SOA mass concentration and yield were only affected by the NO_2 concentration in this study. The $[VOCs]_0/[NO_2]_0$ ratios in this study covered the atmospheric

Table 1
Conditions for the *o*-xylene photooxidation experiment with different $[NO_2]_0$ and RH.

Exp. No.	*o*-xylene	H_2O_2	$[NO_2]_0$	$[VOCs]_0/[NO_2]_0$	RH	SOA mass conc.	$MAC_{\lambda=365\ nm}$
	10^{13} molecule cm^{-3}		ppbv	ppbv/ppbv	%	μg m^{-3}	m^2 g^{-1}
1	1.42	2.53	0	–	17	54.2 ± 1.8	0.23
2			122	4.34	17	74.3 ± 1.3	0.28
3			320	1.65	19	96.3 ± 2.1	0.33
4			893	0.59	17	127.2 ± 0.6	0.43
5			0	–	70	177.7 ± 2.4	0.51
6			121	4.38	72	169.5 ± 1.4	0.61
7			306	1.73	72	153.8 ± 1.2	0.71
8			862	0.61	69	146.5 ± 1.5	0.89

conditions from the clean to the polluted (Zou et al., 2015; Han et al., 2015), thus our experimental conditions are informative to aerosol formation in the real atmosphere. When all reactants were well mixed, the UV-light lamps were turned on and photooxidation was initiated.

2.2. Online instruments

Online instruments measured the NO_2, O_3, and SOA concentrations continuously throughout the photooxidation process. The concentrations of O_3 and NO_2 were measured using an O_3 analyzer (Model 49C, Thermo Electron Corporation, USA) and $NO/NO_2/NO_2$ analyzer (Model 42C, Thermo Electron Corporation, USA), respectively. The formed SOA was measured with a scanning mobility particle sizer (SMPS), which was coupled with a differential mobility analyzer (DMA model 3081, TSI Inc., USA) for the measurement of particle size distributions and a condensation particle counter (CPC model 3776, TSI Inc., USA) for the measurement of concentrations. The sheath gas and sample gas flow rates were 3 L $min^{-1}$and 0.3 L min^{-1}, respectively, in the SMPS. The particle size scan ranged from 13.6 nm to 726.5 nm. A density of 1.4 g cm^{-3} for the aromatic hydrocarbon SOA was assumed when converting the volume concentration of SOA measured by the SMPS to mass concentration (Ng et al., 2007b; Liu et al., 2021b).

The chemical composition of SOA makes it very complicated to identify every photooxidation product. Hence, we used a high-resolution time-of-flight aerosol mass spectrometer (HR-ToF-AMS, Aerodyne Research Inc., USA) to detect the whole SOA chemical composition. It should be pointed out that only the particles with an aerodynamic equivalent diameter below 1 μm could pass through the aerodynamic lens at the injection port and be detected by AMS. Because the W-mode of AMS produces high levels of noise while perform an analysis, only the V-mode of AMS was used in this study. The standard SQUIRREL 1.51H and PIKA 1.10H applications were retrieved from http://cires1.colorado.edu/jimenez-group/ToFAMSResources/ToFSoftware in Igor Pro (WaveMetrics, Inc., USA) for the HR-ToF-AMS data analysis. Notably, for comparability with previous studies, all bulk SOA elemental ratios (i.e. O/C, H/C, and N/C) and mass-to-carbon ratio (OM/OC) were calculated based on the method proposed by Aiken et al. (2008) and Canagaratna et al. (2015).

2.3. SOA collection

After 60 min of reaction, the mass concentration of SOA reached its maximum. The particles were collected on 47 mm polytetrafluoroethylene (PTFE) filters (0.22 μm pore size) with a sampling volume of 3 m^3. PTFE filters were weighed before and after sampling to determine the amount of particles collected. The PTFE filter samples were extracted with 10 mL of methanol under ultrasonication for offline optical property characterization.

The light optical absorption of *o*-xylene derived SOA was analyzed with a UV–Vis spectrometer (P9, Shanghai Mapada, China). In order to eliminate the influence of the amount of SOA collected on the filter on absorbance, the mass absorption coefficient (MAC, m^2 g^{-1}) was used for comparison. The MAC value was calculated using Eq. (1) presented below:

$$MAC_\lambda = (A_\lambda - A_{700}) \cdot \frac{V_l}{V_a \cdot L \cdot M} \cdot \ln(10) \quad (1)$$

where, MAC_λ is the mass absorption coefficient of SOA at the λ wavelength; A_λ and A_{700} are the light absorption intensity at a specific wavelength and background value, respectively; V_l is the volume of methanol with dissolved aerosols; V_a is the volume of the sampled air; L (1 cm) is the optical path length; and M (μg m^{-3}) is the mass concentration of methanol-soluble organic matter.

3. Results and discussion

3.1. SOA mass concentrations

The mass concentrations of *o*-xylene SOA formed with different initial NO_2 concentrations and RH conditions are shown in Fig. 1. The particle wall loss rates were measured at the end of the chamber experiment after the UV-lamps were turned off, and the mass concentration was corrected with the same way of Jiang et al. (2020) and Pathak et al. (2007), which have been described in our previous studies (Liu et al., 2021b; Liu et al., 2022). It needs to be pointed out that the SOA formed in humid conditions was not dried before the SMPS measurement. In order to exclude the contributions of aerosol liquid water (ALW) in particles, a volume growth factor (VGF) of 1.3 was used for the calibration of SOA mass concentration. Here, VGF is defined as the ratio of the particle volume in a humid condition to that after drying (Engelhart et al., 2011). The SOA mass concentrations formed in humid conditions were calibrated based on the VGF in Fig. 1.

In dry conditions, the mass concentration of *o*-xylene derived SOA increased with the increasing initial NO_2 concentration. The SOA mass concentration was 54.2 ± 1.8 μg m^{-3} in the absence of NO_2, and it increased to 74.3 ± 1.3 μg m^{-3}, 96.3 ± 2.1 μg m^{-3}, and 127.2 ± 0.6 μg

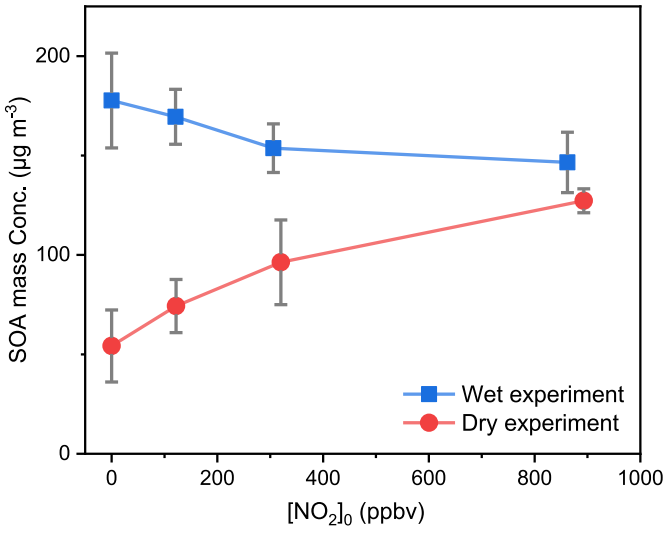

Fig. 1. Mass concentrations of SOA generated by photooxidation of *o*-xylene under different NO_2 concentrations under dry and humid conditions.

m^{-3} when the initial NO_2 concentration was increased to 122 ppbv, 320 ppbv, and 893 ppbv, respectively. A nonlinear trend of an initial increase was followed by a decrease in SOA formation with increasing NO_2 concentration has been widely observed in previous studies (Wildt et al., 2014; Zhao et al., 2018; Liu et al., 2021c). The reaction between NO and RO2, which are formed from the OH-initiated oxidation, which produces higher volatility products, can suppress SOA formation in high NO_x conditions. However, in this study, the SOA formation was not inhibited even when the initial NO_x concentration was increased to the very high level of 893 ppbv. UV light with center wavelength of 254 nm was used to drive H_2O_2 photolysis, while it cannot cause the photolysis of NO_2 to NO as black light in the photooxidation process. In this study, NO_2 was the main form of NO_x, and even in the experiment with high NO_x concentration, the reaction between RO2 and NO was not important and the suppression of SOA formation by NO_x was not observed. The reaction between OH and NO_2 to form nitric acid is one of the most influential reactions in atmospheric chemistry (Mollner et al., 2010). Liu et al. (2021c) reported that nitric acid can participate in the particle-phase, and observed that the concentration ratio of nitrate to SOA increased with increasing NO_x concentration through the NO_2 + OH reaction. More nitrate would therefore increase aerosol acidity. The semi-volatile organic compound products can readily partition into the particle phase through acid-catalyzed heterogeneous reactions via hydration, polymerization, and hemiacetal/acetal formation; thus, this results in the substantial promotion of SOA formation (Jang et al., 2002; Zhao et al., 2018). For different initial NO_2 concentrations, the mass concentration ratio of nitrate ions to SOA ($[NO_3^-]/[Org]$) was compared, as shown in Fig. 2. An increase in the ratio of $[NO_3^-]/[Org]$, which suggested a higher acidity of secondary aerosols, was observed with an increasing initial NO_2 concentration. Hence, the enhanced acid-catalyzed reaction was responsible for the promotion of SOA formation with increased NO_2 concentration.

Sarrafzadeh et al. (2016) suggested that an increase in SOA yield could arise from higher OH concentrations as they promote the formation of low volatility products in β-pinene photooxidation. SOA yield formed from artificial VOCs also appeared to have a strong correlation with OH concentrations, as shown in the studies by Healy et al. (2009) and Qi et al. (2020). A higher oxidation rate results in sufficiently high concentrations of photooxidation products to ensure that more photooxidation products are condensed in the particle-phase and promote SOA formation rather than remaining in the gas-phase, leading to further oxidation. In this study, the H_2O_2 concentration remained constant in different experiments because the same volume of hydrogen peroxide solution was introduced into the chamber, and there was no significant difference in OH concentrations formed from H_2O_2 photolysis. Nitrous acid (HONO) is another important OH precursor in the classical photooxidation process in the atmosphere. HONO could have been generated from the heterogeneous reaction of gas-phase NO_2 on the chamber walls (Finlayson-Pitts et al., 2003; Ge et al., 2019). An

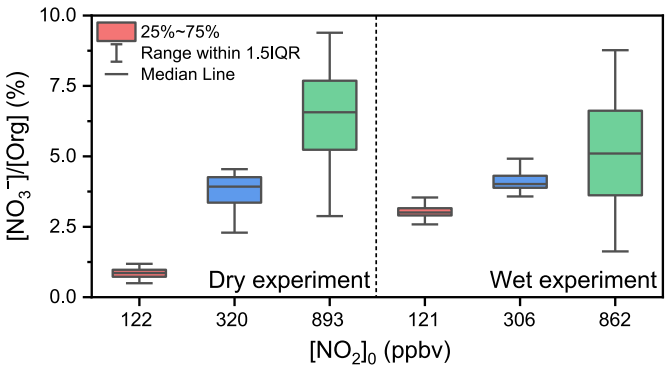

Fig. 2. Mass concentration ratio of nitrate ions to SOA ($[NO_3^-]/[Org]$) for different experimental conditions.

increase in the initial NO_2 concentration would therefore be expected to result in higher OH concentration formed from the photolysis pathway of HONO, and promote SOA formation. Some previous studies have also pointed out that introducing additional HONO could greatly lead to producing higher SOA mass concentrations (Ng et al., 2007b; Healy et al., 2009). For the field observation and model simulation, SOA concentrations were also enhanced when OH radical-formation from the photolysis of HONO, which was generated by the heterogeneous reaction of NO_2, was considered (Liu et al., 2021a; Zhang et al., 2019a). The formation of HONO, which could then produce more OH through photolysis, was responsible for the enhancement of SOA mass concentration to a certain extent in the higher NO_2 concentration conditions. However, Liu et al. (2021a) found that the ratio of $HONO/NO_2$ was in the range of 4%–12% at the urban atmosphere, and the contribution of OH from the photolysis of HONO, which was formed through the heterogeneous reaction of NO_2, contributes to 3.4%–20% of the atmospheric OH. For this diversion ratio of HONO formation and photolysis, in this study, the heterogeneous conversion of NO_2 would provide a maximum of 16 ppbv of OH, which was lower by more than an order of magnitude of the initial H_2O_2 concentration. Considering the SOA mass concentration increased 1.3 times with the initial NO_2 concentration increasing from 0 ppbv to about 900 ppbv, the formation of HONO from heterogeneous conversion of NO_2 was not important for the enhancement of SOA formation when compared with the acid-catalyzed reaction in this study.

The *o*-xylene SOA mass concentrations formed in dry and humid conditions were also compared in this study. Fig. 1 shows that the mass concentrations of *o*-xylene derived SOA at humid conditions were much greater than those at dry conditions. The SOA mass concentrations in dry conditions ranged from 54.2 μg m^{-3} to 127.2 μg m^{-3}. But at high RH conditions, the *o*-xylene derived SOA mass concentration ranged from 146.5 μg m^{-3} to 177.7 μg m^{-3}. The maximum ratio of SOA mass concentration formed in humid conditions to that formed in dry conditions was 3.4, which occurred in the absence of NO_2. A positive effect of RH on SOA formation has also been obtained in other experiments (Kamens et al., 2011; Jia and Xu, 2018; Liu et al., 2019b). The ALW is a key component affecting SOA formation. The soluble oxidation products with high volatility, which are widely present in the gas-phase under dry conditions, were more concentrated on the surface of humid particulates, which increased the mass concentration of SOA (Liu et al., 2019b). Glyoxal and methylglyoxal are important oxidation products of *o*-xylene photooxidation in the atmosphere, but they did not make a significant contribution to SOA formation (only 1–3% for xylene derived SOA) (Nishino et al., 2010). Strong evidence has suggested that the gas phases of both glyoxal and methylglyoxal are uptaken by atmospheric particles, primarily by particle associated water (Volkamer et al., 2009). But Wang et al. (2016b) pointed out that dissolved glyoxal could not completely contribute to the increased mass concentration of SOA under high RH conditions based on Henry's Law constant (Wang et al., 2016b). Aqueous reactions could also have enhanced SOA formation. Dissolved glyoxal can equilibrate to geminal diol or hydrate forms, and rapidly dimerize or trimerize to form oligomers through acid catalyzed hemiacetal formation and aldol condensation (Loeffler et al., 2006; Corrigan et al., 2008; Jia and Xu, 2015; Peters et al., 2021). Hence, at high RH conditions, glyoxal and other soluble substances can produce additional organic compounds via aqueous photochemical reactions in ALW (White et al., 2014; Faust et al., 2017) which do not immediately transform back to the gas-phase, even when SOA is dried. De Haan et al. (2009) showed that more than 30% of the glyoxal mass was preserved in the particle phase when aerosol was dried from aqueous droplets. After the dissolved glyoxal or methylglyoxal reacts, more glyoxal or methylglyoxal was able to consistently participate in the particle phase. Even in the real atmosphere environment photochemical processing and aqueous-phase processing play an important role in SOA production in humid conditions. Based on the formation and evolution characteristics of SOA at urban area, Li et al. (2020) have pointed the enhanced aqueous-phase

oxidation and the partitioning process both contributed to the incorporation of oxygenated species into the particle phase in humid conditions and enhanced the SOA mass concentration, which is consist with our result.

Although an increased RH can promote the formation of *o*-xylene derived SOA, this promoting effect gradually decreased with increasing NO_2 concentration. In contrast to the effect of NO_2 on SOA formation under dry conditions, the mass concentration of *o*-xylene SOA formed in humid conditions gradually decreased with increasing initial NO_2 concentration. As pointed out before, both liquid absorption and liquid phase heterogeneous reactions of glyoxal and methylglyoxal were responsible for increases in SOA mass concentration under high humidity conditions. Nishino et al. (2010) measured the formation yields of glyoxal and methylglyoxal from the gas-phase OH radical-initiated reactions with xylenes, and they found that the yields decreased with increased NO_2 concentration. Their experiment result showed that the glyoxal and methylglyoxal formation yields decreased from 14.3% to 11.5% and from 35.5% to 30.4%, respectively, with the initial NO_2 concentration increasing from 0 ppbv to 893 ppbv. Atkinson and Aschmann (1994) also investigated the effect of NO_2 concentration on the gas-phase products from aromatic hydrocarbons photooxidation, and found that both glyoxal and methylglyoxal decreased with increasing NO_2 concentration in xylene photooxidation process. The atmospheric model results also showed a decrease trend of glyoxal and methylglyoxal yield from the photooxidation of xylene with increasing NO_2 concentration (Bates et al., 2021). The decreased concentrations of glyoxal and methylglyoxal, which could be condensed on humid particles and caused an increase in the SOA mass concentration under high humidity conditions, was weakened with increasing NO_2 concentration. The above results indicated that the decreases in glyoxal and methylglyoxal formation directly caused the decrease in the *o*-xylene derived SOA mass concentration with increasing NO_2 concentrations in humid conditions.

The enhancement of the SOA aging processes at high RH conditions might be another reason that led to different trends in SOA formation with NO_2 under humid and dry conditions. Except for the gas phase reaction, OH radicals can react with particulate organic matter to form small-molecule volatile compounds, which can serve as a sink for SOA (Molina et al., 2004). The OH uptake coefficient is different between low and high RH conditions. In humid conditions, hydrogen bonds between LWC and OH radicals can enhance the attachment of OH radicals and moist SOA surfaces, which would ensure that more OH radicals could react with the condensed organic products (Chan et al., 2014). In addition to its effect on the reaction of OH radicals on the surfaces of SOA, the difference in viscosity and molecular diffusion capacity in the bulk particle phase under different RH conditions would affect the reactivity of OH towards the interiors of SOA. The influence of RH on particle phase viscosity plays an important role in the heterogeneous oxidation of organic aerosols. Moog et al. (1982) showed that the orientation stabilities of molecules in the particle phase were damaged, which could enhance the mobility and decrease the aerosol viscosity of SOA with increases in RH. Smith et al. (2021) also pointed out that the reactive uptake and diffusivity are kinetically inhibited in dry conditions for aromatic SOA because of the high viscosity, and the limitations in the mass transfer rate for uptake are gradually reduced with increasing RH. The heterogeneous reaction of SOA transitioned from diffusion-limited in dry conditions to saturated uptake in humid conditions. The viscosity of condensed organic species would relate to their diffusion coefficient (D_{org}), and would impact the mixing timescale of SOA. The lower the viscosity, the shorter the mixing timescale. In general, in dry conditions, D_{org} is 10^{-15} cm^2 s^{-1} when the corresponding mixing timescale is about 40 min for a 100 nm particle. However, D_{org} increases to 10^{-12} cm^2 s^{-1} in humid conditions, and the mixing timescale for a 100 nm particle is decreased to about 2 s (Koop et al., 2011). An increase in RH could favor the diffusion of OH into the particles. Hence, the aging process of OH radicals may occur throughout the entire particle, not only on the surface of the particle, which would cause an increase in the particle reactivity with increasing RH (Kuwata and Martin, 2012). More OH would react with the condensed organic species to produce small molecule products through fragmentation reactions. Heterogeneous OH oxidation of SOA under low- and high-RH conditions have been studied previously. The aerosol volume loss was more efficient in humid conditions compared to dry conditions (Romonosky et al., 2015; Liu et al., 2019a). The higher net fragmentation values in high-RH conditions were responsible for the loss of SOA through heterogeneous OH oxidation. Li et al. (2018) also pointed out that the aging process of SOA through OH oxidation was accelerated at high RH, and there was a substantial difference in the SOA chemical composition between high RH and low RH conditions. The above findings indicated that an increased mass loss rate of formed SOA occurred with increasing RH at constant OH concentrations. Meanwhile, increased OH concentrations might further increase the mass loss rate of formed SOA in high RH conditions. HONO formation through disproportionation of a heterogeneous reaction of gas-phase NO_2 was increased with increasing initial NO_2 concentration and RH. More OH formed through HONO photolysis, which further enhanced the SOA aging degree under high NO_2 concentrations in humid conditions (Forstner et al., 1997; Zhang et al., 2019b). Due to these reasons, a decreased SOA mass concentration was observed with an increase in NO_2 concentration in high RH conditions. It should pointed out here that NO_2 even suppressed *o*-xylene derived SOA formation in humid conditions, the SOA mass concentration in humid conditions was still higher than that in dry conditions, even with high NO_2 levels.

3.2. SOA light absorption

Optical absorption is an important property for evaluating the influence of SOA on solar radiation and climate effects. The $MAC_{\lambda = 365\ nm}$ of *o*-xylene derived SOA with different NO_2 concentrations and RH conditions was investigated in this section and is shown in Fig. 3.

As shown in Fig. 3, an increased $MAC_{\lambda = 365\ nm}$ value increased with NO_2 concentration in both low and high RH conditions. $MAC_{\lambda = 365\ nm}$ of the *o*-xylene derived SOA was 0.23 m^2 g^{-1} in the absence of NO_2, and it increased to 0.43 m^2 g^{-1} when the initial concentration of NO_2 was increased to 893 ppbv in dry conditions. In humid conditions, $MAC_{\lambda = 365\ nm}$ increased from 0.51 m^2 g^{-1} to 0.89 m^2 g^{-1} as the initial NO_2 concentration increased from 0 ppbv to 862 ppbv. The effect of increasing NO_2 on the SOA light-absorbing ability was in accordance with previous studies (Xie et al., 2017; Liu et al., 2022). However, the

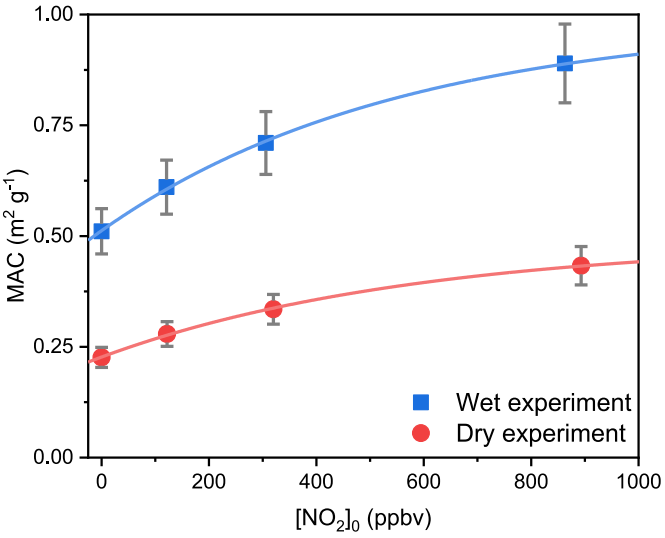

Fig. 3. Evolution of $MAC_{\lambda = 365\ nm}$ of *o*-xylene SOA formed with different initial NO_2 concentrations at both humid and dry conditions.

$MAC_{\lambda = 365\ nm}$ of *o*-xylene derived SOA did not have a linear relationship with initial NO_2 concentration. The increase in the ratio of $MAC_{\lambda = 365\ nm}$ with NO_2 gradually decreased with increasing NO_2 concentration. In the absence of NO_2, the increase in the ratio of $MAC_{\lambda = 365\ nm}$ with NO_2 was 4.4×10^{-4} m^2 g^{-1} $ppbv^{-1}$ in dry conditions and 9.0×10^{-4} m^2 g^{-1} $ppbv^{-1}$ in humid conditions. In dry conditions, when the initial NO_2 concentrations increased to 122 ppbv, 320 ppbv, and 893 ppbv, the increase in the ratio of $MAC_{\lambda = 365\ nm}$ with NO_2 was decreased to 3.6×10^{-4} m^2 g^{-1} $ppbv^{-1}$, 2.7×10^{-4} m^2 g^{-1} $ppbv^{-1}$, and 8.2×10^{-4} m^2 g^{-1} $ppbv^{-1}$, respectively. In humid conditions, when the initial NO_2 concentration increased to 121 ppbv, 306 ppbv, and 862 ppbv, the increase in the ratio of $MAC_{\lambda = 365\ nm}$ with NO_2 was decreased to 7.0×10^{-4} m^2 g^{-1} $ppbv^{-1}$, 4.8×10^{-4} m^2 g^{-1} $ppbv^{-1}$, and 1.1×10^{-4} m^2 g^{-1} $ppbv^{-1}$, respectively.

In addition, for the experiment with similar initial NO_2 concentrations, the $MAC_{\lambda = 365\ nm}$ was higher for *o*-xylene SOA formed in humid conditions than that formed in dry conditions. The $MAC_{\lambda = 365\ nm}$ of SOA increased 2.1–2.3 times from the low RH to high RH conditions. It is important to point out that, in dry conditions, even if the initial NO_2 concentration was increased to 893 ppbv, which is almost impossibly high for real environments, the $MAC_{\lambda = 365\ nm}$ of *o*-xylene derived SOA was 0.43 m^2 g^{-1}, which was still lower than that formed in the absence of NO_2 under a high RH condition (0.51 m^2 g^{-1}). Clearly, RH is an important factor that strongly affects the absorbance of SOA.

3.3. SOA chemical composition

The chemical composition of SOA generated through OH oxidation of *o*-xylene with different RH and NO_2 concentrations was investigated online with a HR-ToF-AMS. In previous photooxidation studies, most SOA formation mechanisms were obtained based on the chemical compositions, which were detected through offline mass spectrometry (Klodt et al., 2022; Shen et al., 2018; Romonosky et al., 2015). Relative changes in the SOA chemical composition occur through the photooxidation process, which is important in understanding of the mechanism of SOA formation, but is often neglected. The changes in mass spectra are considered to be a function of OH exposure. Here, the average carbon oxidation state ($OS_C \approx 2$ O/C–H/C) was used to describe the changes in the degree of oxidation of *o*-xylene derived SOA during the photooxidation process. The different OS_C values and change trends observed for *o*-xylene SOA formed in different NO_2 concentrations in dry and humid conditions are shown in Fig. 4.

For photooxidation in dry condition, the OS_C of *o*-xylene derived SOA decreased with increasing initial NO_2 concentration. This result suggested that some high volatility oxidation products with lower OS_C values, which were present in the gas phase in experiments without NO_2, was able to participate in the particle phase in the presence of NO_2 through the acid-catalyzed reactions (Kroll et al., 2011). The lower OS_C value for photooxidation with a higher initial NO_2 concentration also illustrated that the acid-catalyzed reaction was enhanced by increased NO_2 concentrations, which proved that the promotion of SOA formation was attributed to the increase in acid-catalyzed reactions, as pointed out in Section 3.1.

When we compared the OS_C of SOA formed in dry and humid conditions in the absence of NO_2, the OS_C value was lower for SOA formed in humid conditions than in dry conditions. This result also suggested that some water-soluble compounds with lower OS_C and high volatility were present in the gas phase in dry conditions, which could increase the SOA mass concentration via uptake or aqueous reactions in aerosol water in high RH conditions (Ng et al., 2007b; Jia and Xu, 2018). In contrast to dry conditions, the OS_C value for *o*-xylene SOA did not change appreciably with different initial NO_2 concentrations in humid conditions. However, the change rate of OS_C with time increased with increasing NO_2 concentration in humid conditions. The OS_C change rates of SOA for experiments with initial NO_2 concentrations of 121 ppbv, 306 ppbv, and 862 ppbv were increased by 12.8%, 20.6%, and 59.1%, respectively, relative to when NO_2 was absent in humid conditions. The rate of change of OS_C reflects the aging rate of SOA (Han et al., 2016). Thus, the aging process of *o*-xylene derived SOA was promoted by increases in the NO_2 concentration in humid conditions, and the enhanced aging process was mainly responsible for the suppression of SOA formation by NO_2 in humid conditions. Although an increased NO_2 concentration can promote OH concentration by increasing the formation of HONO, the OS_C change rate of SOA in experiments in dry condition was not affected by increases in the NO_2 concentration. Both OH concentration and reactive activation of OH with SOA were key factors affecting SOA aging. The different OS_C change rates of SOA with different initial NO_2 concentrations in dry or humid conditions also illustrated that the aging process of SOA was restricted in dry conditions because of the low mobility and high viscosity of SOA, which inhibited the diffusion of OH into SOA and the aging reaction of OH with the internal organic components of SOA. In humid conditions, the mobility of SOA was not the limiting factor for OH reactions with organic components of SOA, as pointed out in Section 3.2, and the aging process of *o*-xylene derived SOA was directly affected by the OH concentration. The above results indicated that the aging process of SOA with increases in the OH concentration was not consistent between dry and humid conditions, and the aging process was faster in high RH conditions.

It has been pointed out that NOCs can be formed through photooxidation in the presence of NO_2, and NOCs are important light-absorbing components in SOA (Lee et al., 2014; Laskin et al., 2015; Li et al., 2021). The relationship between $MAC_{\lambda = 365\ nm}$ and the content of NOC fragments in the total SOA mass under different NO_2 concentrations in both dry and humid conditions is shown in Fig. 5. At similar NO_2 concentrations, the NOC content of *o*-xylene SOA formed in humid conditions was higher than that formed in dry conditions. This shows that an increased RH is beneficial to the formation of nitrogenous organic matter in SOA. Li et al. (2021) analyzed light absorption and chromophore properties of SOA in the winter of Beijing, and they indicated the aqueous-phase pathways were more important for elevated formation of

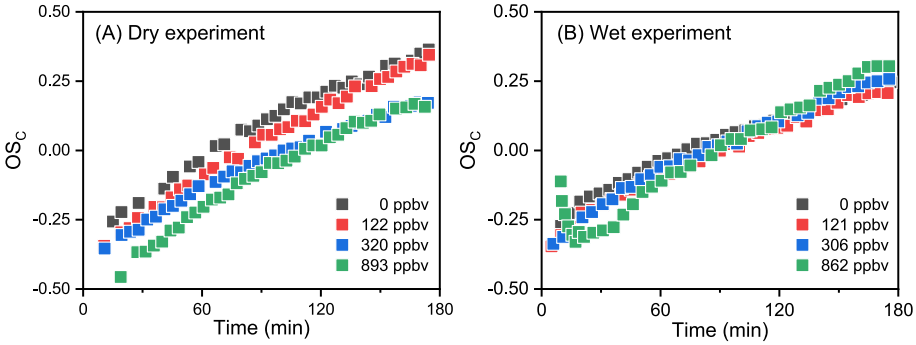

Fig. 4. Evolution of OS_C values for *o*-xylene SOA formed at different initial NO_2 concentrations in dry (A) and humid (B) conditions.

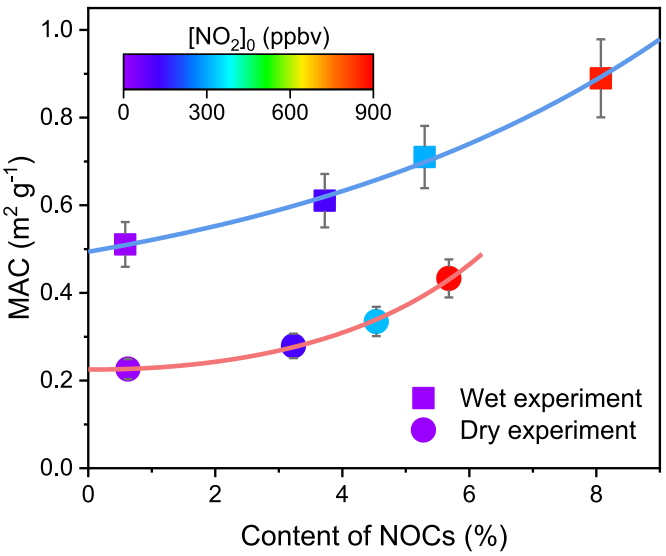

Fig. 5. Relationship between $MAC_{\lambda = 365\ nm}$ and NOCs of *o*-xylene SOA under different $[NO_2]_0$ conditions in both dry and humid conditions.

NOCs under a higher RH condition. Previous chamber studies also pointed out that more NOCs were formed though atmospheric aqueous phases in the presence of NO_2 (Smith et al., 2016; He et al., 2019). The increased NOC content with increased RH observed here was in agreement with those field and chamber studies, which indicated that the atmospheric aqueous phase reactions are more important than gas phase reactions for NOC formation and increase the content of NOCs in SOA. Meanwhile, considering that the SOA mass concentration was higher in humid conditions than in dry conditions, the increase in the amount of NOCs was even more significant in high RH conditions. When compared with dry conditions, the NOC content of *o*-xylene SOA formed in humid conditions was higher by 15.3%, 16.8%, and 42.1% with initial NO_2 concentrations of about 120 ppbv, 320 ppbv, and 900 ppbv, respectively. However, the amount of NOC fragments increased by 45.2%, 34.8%, and 63.0% in humid conditions, more than in dry conditions, in the experiments with initial NO_2 concentrations of about 120 ppbv, 320 ppbv, and 900 ppbv, respectively.

Fig. 5 shows that the $MAC_{\lambda = 365\ nm}$ of *o*-xylene derived SOA increased along with the content of NOCs in both dry and humid conditions, but $MAC_{\lambda = 365\ nm}$ was not linearly related with the NOC content of *o*-xylene SOA. The ratio of $MAC_{\lambda = 365\ nm}$ to NOC content increased with increasing initial NO_2 concentration, and the enhancement of this ratio was more obvious in dry conditions than humid conditions. When comparing between dry and humid conditions, the $MAC_{\lambda = 365\ nm}$ of SOA formed in humid conditions was much higher than that in dry conditions. Based on the above findings, it appeared that the content of NOCs is not the only factor that affects the light absorption of SOA. Other types of oxidation products could also increase the absorption of SOA in humid and high NO_2 conditions.

Humic-like substances (HULIS) are important light-absorbing substances in SOA (Hoffer et al., 2006; Laskin et al., 2015; Wu et al., 2022). Hoffer et al. (2006) also pointed out that HULIS could partially account for the unexplained fraction of light absorption observed in the troposphere. HULIS can be produced through aqueous processing, oligomerization of water-soluble organics, and multiphase chemistry reactions of organic products derived from photooxidation of anthropogenic VOCs (Herckes et al., 2013; Paglione et al., 2014). Zhang et al. (2020) also found that an increased RH could enhance the optical properties of SOA formed from OH oxidation of aromatic VOCs, and the formation of oligomers through liquid phase reactions might be responsible for the enhancement of light absorption in humid conditions. Based on the above findings, we suspected that the increased ratio of $MAC_{\lambda = 365\ nm}$ to NOC content at a high NO_2 concentration was caused by HULIS formation through a heterogeneous acid-catalyzed reaction, and enhanced HULIS formation through a liquid reaction might be responsible for the higher $MAC_{\lambda = 365\ nm}$ of *o*-xylene SOA formed in humid conditions with the same NOC content. However, the reaction mechanism and formation yield of HULIS from aromatic hydrocarbon was not considered in this study and should be explored in the future.

4. Conclusion

The mass concentration and light absorption of *o*-xylene SOA formed from OH photooxidation with different initial NO_2 concentrations were studied in both humid and dry conditions using a chamber simulation technique. When compared with the dry condition, the mass concentration of *o*-xylene derived SOA was enhanced in humid conditions. In the absence of NO_2, *o*-xylene SOA was higher by 3.4 times in the SOA formed in humid conditions compared to that formed in dry conditions. The increased SOA mass concentration under humid conditions was mainly due to dissolution of water-soluble products (e.g. glyoxal and methylglyoxal) and aqueous reactions. This study observed that NO_2 had two opposite effects on SOA formation depending on whether conditions were dry or humid. When the initial NO_2 concentration was increased from 0 ppbv to about 900 ppbv, *o*-xylene SOA mass concentration increased from 54.2 μg m^{-3} to 127.2 μg m^{-3} in dry conditions, but decreased from 230.7 μg m^{-3} to 190.3 μg m^{-3} in humid conditions. The AMS results showed that lower oxidation products participated in the particle phase through acid-catalyzed heterogeneous reactions resulting in the promotion of SOA formation at a high NO_2 concentration in dry conditions, however, an increase in the aging process was responsible for the decreased SOA mass concentration with elevated NO_2 in humid conditions.

Light absorption of *o*-xylene SOA was enhanced with increased NO_2 concentration and RH conditions. The highest $MAC_{\lambda = 365\ nm}$ of 0.89 m^2 g^{-1} was obtained in humid conditions with an initial NO_2 concentration of 862 ppbv, and was about 4 times higher than that obtained in dry conditions without NO_2. The content of NOC fragments also increased with increases in NO_2 concentrations and RH, but it did not show a robust linear correlation with $MAC_{\lambda = 365\ nm}$. This result suggested that NOCs make an important contribution to light absorption of *o*-xylene SOA. But beyond that, we suspected that HULIS formed through heterogeneous acid-catalyzed reactions at a high NO_2 concentration and liquid reactions contributed to the extra light absorption of *o*-xylene SOA formed at high NO_2 and RH conditions.

Author contributions

SL and GW designed the experiment. SL, YW and XX conducted the experiments. SL, YW, and GW performed the data interpretation. SL and GW wrote the paper.

Declaration of competing interest

The authors declare that they have no known competing financial interests or personal relationships that could have appeared to influence the work reported in this paper.

Data availability

No data was used for the research described in the article.

Acknowledgments

This work was financially supported by the National Natural Science Foundation of China (No. 42130704, 42005088), the China Postdoctoral Science Foundation (No. 2022T150215), Shanghai Science and Technology Innovation Action Plan (20dz1204000) and ECNU Happiness

Flower program.

References

Aiken, A.C., Decarlo, P.F., Kroll, J.H., Worsnop, D.R., Huffman, J.A., Docherty, K.S., Ulbrich, I.M., Mohr, C., Kimmel, J.R., Sueper, D., Sun, Y., Zhang, Q., Trimborn, A., Northway, M., Ziemann, P.J., Canagaratna, M.R., Onasch, T.B., Alfarra, M.R., Prevot, A.S., Dommen, J., Duplissy, J., Metzger, A., Baltensperger, U., Jimenez, J.L., 2008. O/C and OM/OC ratios of primary, secondary, and ambient organic aerosols with high-resolution time-of-flight aerosol mass spectrometry. Environ. Sci. Technol. 42, 4478–4485. https://doi.org/10.1021/es703009q.

Aruffo, E., Wang, J., Ye, J., Ohno, P., Qin, Y., Stewart, M., McKinney, K., Di Carlo, P., Martin, S.T., 2022. Partitioning of organonitrates in the production of secondary organic aerosols from α-pinene photo-oxidation. Environ. Sci. Technol. https://doi.org/10.1021/acs.est.1c08380.

Atkinson, R., Aschmann, S.M., 1994. Products of the gas-phase reactions of aromatic hydrocarbons: effect of NO_2 concentration. Int. J. Chem. Kinet. 26, 929–944. https://doi.org/10.1002/kin.550260907.

Bates, K.H., Jacob, D.J., Li, K., Ivatt, P.D., Evans, M.J., Yan, Y., Lin, J., 2021. Development and evaluation of a new compact mechanism for aromatic oxidation in atmospheric models. Atmos. Chem. Phys. 21, 18351–18374. https://doi.org/10.5194/acp-21-18351-2021.

Bianchi, F., Kurten, T., Riva, M., Mohr, C., Rissanen, M.P., Roldin, P., Berndt, T., Crounse, J.D., Wennberg, P.O., Mentel, T.F., Wildt, J., Junninen, H., Jokinen, T., Kulmala, M., Worsnop, D.R., Thornton, J.A., Donahue, N., Kjaergaard, H.G., Ehn, M., 2019. Highly oxygenated organic molecules (HOM) from gas-phase autoxidation involving peroxy radicals: a key contributor to atmospheric aerosol. Chem. Rev. 119, 3472–3509. https://doi.org/10.1021/acs.chemrev.8b00395.

Canagaratna, M.R., Jimenez, J.L., Kroll, J.H., Chen, Q., Kessler, S.H., Massoli, P., Hildebrandt Ruiz, L., Fortner, E., Williams, L.R., Wilson, K.R., Surratt, J.D., Donahue, N.M., Jayne, J.T., Worsnop, D.R., 2015. Elemental ratio measurements of organic compounds using aerosol mass spectrometry: characterization, improved calibration, and implications. Atmos. Chem. Phys. 15, 253–272. https://doi.org/10.5194/acp-15-253-2015.

Chan, M.N., Zhang, H.F., Goldstein, A.H., Wilson, K.R., 2014. Role of water and phase in the heterogeneous oxidation of solid and aqueous succinic acid aerosol by hydroxyl radicals. J. Phys. Chem. C 118, 28978–28992. https://doi.org/10.1021/jp5012022.

Charan, S.M., Huang, Y., Seinfeld, J.H., 2019. Computational simulation of secondary organic aerosol formation in laboratory chambers. Chem. Rev. 119, 11912–11944. https://doi.org/10.1021/acs.chemrev.9b00358.

Chu, B.W., Zhang, X., Liu, Y.C., He, H., Sun, Y., Jiang, J.K., Li, J.H., Hao, J.M., 2016. Synergetic formation of secondary inorganic and organic aerosol: effect of SO_2 and NH_3 on particle formation and growth. Atmos. Chem. Phys. 16, 14219–14230. https://doi.org/10.5194/acp-16-14219-2016.

Corrigan, A.L., Hanley, S.W., De Haan, D.O., 2008. Uptake of glyoxal by organic and Inorganic aerosol. Environ. Sci. Technol. 42, 4428–4433. https://doi.org/10.1021/es7032394.

De Haan, D.O., Corrigan, A.L., Tolbert, M.A., Jimenez, J.L., Wood, S.E., Turley, J.J., 2009. Secondary organic aerosol formation by self-reactions of methylglyoxal and glyoxal in evaporating droplets. Environ. Sci. Technol. 43, 8184–8190. https://doi.org/10.1021/es902152t.

Eddingsaas, N.C., Loza, C.L., Yee, L.D., Chan, M., Schilling, K.A., Chhabra, P.S., Seinfeld, J.H., Wennberg, P.O., 2012. α-pinene photooxidation under controlled chemical conditions - Part 2: SOA yield and composition in low- and high-NOx environments. Atmos. Chem. Phys. 12, 7413–7427. https://doi.org/10.5194/acp-12-7413-2012.

Engelhart, G.J., Hildebrandt, L., Kostenidou, E., Mihalopoulos, N., Donahue, N.M., Pandis, S.N., 2011. Water content of aged aerosol. Atmos. Chem. Phys. 11, 911–920. https://doi.org/10.5194/acp-11-911-2011.

Faust A., J., Wong P., J., Lee K., A., Abbatt P., J., 2017. Role of aerosol liquid water in secondary organic aerosol formation from volatile organic compounds. Environ. Sci. Technol. 51, 1405–1413. https://doi.org/10.1021/acs.est.6b04700.

Finlayson-Pitts, B.J., Wingen, L.M., Sumner, A.L., Syomin, D., Ramazan, K.A., 2003. The heterogeneous hydrolysis of NO_2 in laboratory systems and in outdoor and indoor atmospheres: an integrated mechanism. Phys. Chem. Chem. Phys. 5, 223–242. https://doi.org/10.1039/b208564j.

Forstner, H.J.L., Flagan, R.C., Seinfeld, J.H., 1997. Secondary organic aerosol from the photooxidation of aromatic hydrocarbons: molecular composition. Environ. Sci. Technol. 31, 1345–1358. https://doi.org/10.1021/es9605376.

Gaubert, B., Bouarar, I., Doumbia, T., Liu, Y., Stavrakou, T., Deroubaix, A., Darras, S., Elguindi, N., Granier, C., Lacey, F., Muller, J.F., Shi, X., Tilmes, S., Wang, T., Brasseur, G.P., 2021. Global changes in secondary atmospheric pollutants during the 2020 COVID-19 pandemic. J. Geophys. Res. Atmos. 126, e2020JD034213 https://doi.org/10.1029/2020JD034213.

Ge, S.S., Wang, G.H., Zhang, S., Li, D.P., Xie, Y.N., Wu, C., Yuan, Q., Chen, J., Zhang, H., 2019. Abundant NH_3 in China enhances atmospheric HONO production by promoting the heterogeneous reaction of SO_2 with NO_2. Environ. Sci. Technol. 53, 14339–14347. https://doi.org/10.1021/acs.est.9b04196.

George, C., Ammann, M., D'Anna, B., Donaldson, D.J., Nizkorodov, S.A., 2015. Heterogeneous photochemistry in the atmosphere. Chem. Rev. 115, 4218–4258. https://doi.org/10.1021/cr500648z.

Gu, S., Guenther, A., Faiola, C., 2021. Effects of anthropogenic and biogenic volatile organic compounds on Los Angeles air quality. Environ. Sci. Technol. 55, 12191–12201. https://doi.org/10.1021/acs.est.1c01481.

Han, T., Qiao, L., Zhou, M., Qu, Y., Du, J., Liu, X., Lou, S., Chen, C., Wang, H., Zhang, F., Yu, Q., Wu, Q., 2015. Chemical and optical properties of aerosols and their interrelationship in winter in the megacity Shanghai of China. J. Environ. Sci. 27, 59–69. https://doi.org/10.1016/j.jes.2014.04.018.

Han, Z.W., Xie, Z.X., Wang, G.H., Zhang, R.J., Tao, J., 2016. Modeling organic aerosols over east China using a volatility basis-set approach with aging mechanism in a regional air quality model. Atmos. Environ. 124, 186–198. https://doi.org/10.1016/j.atmosenv.2015.05.045.

He, L., Schaefer, T., Otto, T., Kroflic, A., Herrmann, H., 2019. Kinetic and theoretical study of the atmospheric aqueous-phase reactions of OH radicals with methoxyphenolic compounds. J. Phys. Chem. A 123, 7828–7838. https://doi.org/10.1021/acs.jpca.9b05696.

Healy, R.M., Temime, B., Kuprovskyte, K., Wenger, J.C., 2009. Effect of relative humidity on gas/particle partitioning and aerosol mass yield in the photooxidation of *p*-xylene. Environ. Sci. Technol. 43, 1884–1889. https://doi.org/10.1021/es802404z.

Herckes, P., Valsaraj, K.T., Collett, J.L., 2013. A review of observations of organic matter in fogs and clouds: origin, processing and fate. Atmos. Res. 132–133, 434–449. https://doi.org/10.1016/j.atmosres.2013.06.005.

Hoffer, A., Gelencsér, A., Guyon, P., Kiss, G., Schmid, O., Frank, G.P., Artaxo, P., Andreae, M.O., 2006. Optical properties of humic-like substances (HULIS) in biomass-burning aerosols. Atmos. Chem. Phys. 6, 3563–3570. https://doi.org/10.5194/acp-6-3563-2006.

Huang, X.F., Dai, J., Zhu, Q., Yu, K., Du, K., 2020. Abundant biogenic oxygenated organic aerosol in atmospheric coarse particles: plausible sources and atmospheric implications. Environ. Sci. Technol. 54, 1425–1430. https://doi.org/10.1021/acs.est.9b06311.

Jang, M., Czoschke, N.M., Lee, S., Kamens, R.M., 2002. Heterogeneous atmospheric aerosol production by acid-catalyzed particle-phase reactions. Science 298, 814–817. https://doi.org/10.1126/science.1075798.

Jia, L., Xu, Y.F., 2015. Ozone and secondary organic aerosol formation from Ethylene-NO_x-NaCl irradiations under different relative humidity conditions. J. Environ. Sci. 73, 81–100. https://doi.org/10.1007/s10874-015-9317-1.

Jia, L., Xu, Y.F., 2018. Different roles of water in secondary organic aerosol formation from toluene and isoprene. Atmos. Chem. Phys. 18, 8137–8154. https://doi.org/10.5194/acp-18-8137-2018.

Jiang, X.T., Lv, C., You, B., Liu, Z.Y., Wang, X.F., Du, L., 2020. Joint impact of atmospheric SO_2 and NH_3 on the formation of nanoparticles from photo-oxidation of a typical biomass burning compound. Environ Sci-Nano 7, 2532–2545. https://doi.org/10.1039/d0en00520g.

Kamens, R.M., Zhang, H., Chen, E.H., Zhou, Y., Parikh, H.M., Wilson, R.L., Galloway, K.E., Rosen, E.P., 2011. Secondary organic aerosol formation from toluene in an atmospheric hydrocarbon mixture: water and particle seed effects. Atmos. Environ. 45, 2324–2334. https://doi.org/10.1016/j.atmosenv.2010.11.007.

Klodt, A.L., Adamek, M., Dibley, M., Nizkorodov, S.A., O'Brien, R.E., 2022. Effects of the sample matrix on the photobleaching and photodegradation of toluene-derived secondary organic aerosol compounds. Atmos. Chem. Phys. 22, 10155–10171. https://doi.org/10.5194/acp-22-10155-2022.

Koop, T., Bookhold, J., Shiraiwa, M., Poschl, U., 2011. Glass transition and phase state of organic compounds: dependency on molecular properties and implications for secondary organic aerosols in the atmosphere. Phys. Chem. Chem. Phys. 13, 19238–19255. https://doi.org/10.1039/c1cp22617g.

Kroll, J.H., Donahue, N.M., Jimenez, J.L., Kessler, S.H., Canagaratna, M.R., Wilson, K.R., Altieri, K.E., Mazzoleni, L.R., Wozniak, A.S., Bluhm, H., Mysak, E.R., Smith, J.D., Kolb, C.E., Worsnop, D.R., 2011. Carbon oxidation state as a metric for describing the chemistry of atmospheric organic aerosol. Nat. Chem. 3, 133–139. https://doi.org/10.1038/nchem.948.

Kuwata, M., Martin, S.T., 2012. Phase of atmospheric secondary organic material affects its reactivity. Proc. Natl. Acad. Sci. U.S.A. 109, 17354–17359. https://doi.org/10.1073/pnas.1209071109.

Laskin, A., Laskin, J., Nizkorodov, S.A., 2015. Chemistry of atmospheric brown carbon. Chem. Rev. 115, 4335–4382. https://doi.org/10.1021/cr5006167.

Lee, H.J., Aiona, P.K., Laskin, A., Laskin, J., Nizkorodov, S.A., 2014. Effect of solar radiation on the optical properties and molecular composition of laboratory proxies of atmospheric brown carbon. Environ. Sci. Technol. 48, 10217–10226. https://doi.org/10.1021/es502515r.

Li, J.Y., Liu, Z.R., Gao, W.K., Tang, G.Q., Hu, B., Ma, Z.Q., Wang, Y.S., 2020. Insight into the formation and evolution of secondary organic aerosol in the megacity of Beijing, China. Atmos. Environ. 220, 117070 https://doi.org/10.1016/j.atmosenv.2019.117070. ARTN 117070.

Li, Q., Jiang, J., Afreh, I.K., Barsanti, K.C., Cocker Iii, D.R., 2022. Secondary organic aerosol formation from camphene oxidation: measurements and modeling. Atmos. Chem. Phys. 22, 3131–3147. https://doi.org/10.5194/acp-22-3131-2022.

Li, X.R., Zhao, Q., Yang, Y., Zhao, Z.Y., Liu, Z.R., Wen, T.X., Hu, B., Wang, Y.S., Wang, L.L., Wang, G.H., 2021. Composition and sources of brown carbon aerosols in megacity Beijing during the winter of 2016. Atmos. Res. 262 https://doi.org/10.1016/j.atmosres.2021.105773. ARTN 105773.

Li, Z., Smith, K.A., Cappa, C.D., 2018. Influence of relative humidity on the heterogeneous oxidation of secondary organic aerosol. Atmos. Chem. Phys. 18, 14585–14608. https://doi.org/10.5194/acp-18-14585-2018.

Liu, J.Y., Liu, Z.R., Ma, Z.Q., Yang, S., Yao, D., Zhao, S., Hu, B., Tang, G., Sun, J., Cheng, M.T., Xu, Z.J., Wang, Y.S., 2021a. Detailed budget analysis of HONO in Beijing, China: implication on atmosphere oxidation capacity in polluted megacity. Atmos. Environ. 244, 117957 https://doi.org/10.1016/j.atmosenv.2020.117957.

Liu, S.J., Jiang, X.T., Tsona, N.T., Lv, C., Du, L., 2019a. Effects of NO_x, SO_2 and RH on the SOA formation from cyclohexene photooxidation. Chemosphere 216, 794–804. https://doi.org/10.1016/j.chemosphere.2018.10.180.

Liu, S.J., Tsona, N.T., Zhang, Q., Jia, L., Xu, Y.F., Du, L., 2019b. Influence of relative humidity on cyclohexene SOA formation from OH photooxidation. Chemosphere 231, 478–486. https://doi.org/10.1016/j.chemosphere.2019.05.131.

Liu, S.J., Huang, D.D., Wang, Y.Q., Zhang, S., Liu, X.D., Wu, C., Du, W., Wang, G.H., 2021b. Synergetic effects of NH_3 and NO_x on the production and optical absorption of secondary organic aerosol formation from toluene photooxidation. Atmos. Chem. Phys. 21, 17759–17773. https://doi.org/10.5194/acp-21-17759-2021.

Liu, S.J., Wang, Y.Q., Wang, G.H., Zhang, S., Li, D.P., Du, L., Wu, C., Du, W., Ge, S.S., 2021c. Enhancing effect of NO_2 on the formation of light-absorbing secondary organic aerosols from toluene photooxidation. Sci. Total Environ. 794, 148714 https://doi.org/10.1016/j.scitotenv.2021.148714.

Liu, S.J., Liu, X., Wang, Y., Zhang, S., Wu, C., Du, W., Wang, G., 2022. Effect of NO_x and RH on the secondary organic aerosol formation from toluene photooxidation. J. Environ. Sci. 114, 1–9. https://doi.org/10.1016/j.jes.2021.06.017.

Loeffler, K.W., Koehler, C.A., Paul, N.M., De Haan, D.O., 2006. Oligomer formation in evaporating aqueous glyoxal and methyl glyoxal solutions. Environ. Sci. Technol. 40, 6318. https://doi.org/10.1021/es060810w, 6123.

Molina, M.J., Ivanov, A.V., Trakhtenberg, S., Molina, L.T., 2004. Atmospheric evolution of organic aerosol. Geophys. Res. Lett. 31 https://doi.org/10.1029/2004gl020910. Artn L22104.

Mollner, A.K., Valluvadasan, S., Feng, L., Sprague, M.K., Okumura, M., Milligan, D.B., Bloss, W.J., Sander, S.P., Martien, P.T., Harley, R.A., McCoy, A.B., Carter, W.P., 2010. Rate of gas phase association of hydroxyl radical and nitrogen dioxide. Science 330, 646–649. https://doi.org/10.1126/science.1193030.

Moog, R.S., Ediger, M.D., Boxer, S.G., Fayer, M.D., 1982. Viscosity dependence of the rotational reorientation of rhodamine B in mono- and polyalcohols. Picosecond transient grating experiments. J. Phys. Chem. 86, 4694–4700. https://doi.org/10.1021/j100221a011.

Ng, N.L., Chhabra, P.S., Chan, A.W.H., Surratt, J.D., Kroll, J.H., Kwan, A.J., McCabe, D. C., Wennberg, P.O., Sorooshian, A., Murphy, S.M., Dalleska, N.F., Flagan, R.C., Seinfeld, J.H., 2007a. Effect of NOx level on secondary organic aerosol (SOA) formation from the photooxidation of terpenes. Atmos. Chem. Phys. 7, 5159–5174. https://doi.org/10.5194/acp-7-5159-2007.

Ng, N.L., Kroll, J.H., Chan, A.W.H., Chhabra, P.S., Flagan, R.C., Seinfeld, J.H., 2007b. Secondary organic aerosol formation from *m*-xylene, toluene, and benzene. Atmos. Chem. Phys. 7, 3909–3922. https://doi.org/10.5194/acp-7-3909-2007.

Nishino, N., Arey, J., Atkinson, R., 2010. Formation yields of glyoxal and methylglyoxal from the gas-phase OH radical-initiated reactions of toluene, xylenes, and trimethylbenzenes as a function of NO_2 concentration. J. Phys. Chem. A 114, 10140–10147. https://doi.org/10.1021/jp105112h.

Noziere, B., Kalberer, M., Claeys, M., Allan, J., D'Anna, B., Decesari, S., Finessi, E., Glasius, M., Grgic, I., Hamilton, J.F., Hoffmann, T., Iinuma, Y., Jaoui, M., Kahnt, A., Kampf, C.J., Kourtchev, I., Maenhaut, W., Marsden, N., Saarikoski, S., Schnelle-Kreis, J., Surratt, J.D., Szidat, S., Szmigielski, R., Wisthaler, A., 2015. The molecular identification of organic compounds in the atmosphere: state of the art and challenges. Chem. Rev. 115, 3919–3983. https://doi.org/10.1021/cr5003485.

Offenberg, J.H., Lewandowski, M., Edney, E.O., Kleindienst, T.E., Jaoui, M., 2009. Influence of aerosol acidity on the formation of secondary organic aerosol from biogenic precursor hydrocarbons. Environ. Sci. Technol. 43, 7742–7747. https://doi.org/10.1021/es901538e.

Paglione, M., Kiendler-Scharr, A., Mensah, A.A., Finessi, E., Giulianelli, L., Sandrini, S., Facchini, M.C., Fuzzi, S., Schlag, P., Piazzalunga, A., Tagliavini, E., Henzing, J.S., Decesari, S., 2014. Identification of humic-like substances (HULIS) in oxygenated organic aerosols using NMR and AMS factor analyses and liquid chromatographic techniques. Atmos. Chem. Phys. 14, 25–45. https://doi.org/10.5194/acp-14-25-2014.

Pathak, R.K., Stanier, C.O., Donahue, N.M., Pandis, S.N., 2007. Ozonolysis of alpha-pinene at atmospherically relevant concentrations: temperature dependence of aerosol mass fractions (yields). J. Geophys. Res. Atmos. 112 https://doi.org/10.1029/2006jd007436. Artn D03201.

Peters, J.H., Dette, H.P., Koop, T., 2021. Glyoxal as a potential source of highly viscous aerosol particles. ACS Earth Space Chem 5, 3324–3337. https://doi.org/10.1021/acsearthspacechem.1c00245.

Qi, X., Zhu, S., Zhu, C., Hu, J., Lou, S., Xu, L., Dong, J., Cheng, P., 2020. Smog chamber study of the effects of NO_x and NH_3 on the formation of secondary organic aerosols and optical properties from photo-oxidation of toluene. Sci. Total Environ. 727, 138632 https://doi.org/10.1016/j.scitotenv.2020.138632.

Romonosky, D.E., Laskin, A., Laskin, J., Nizkorodov, S.A., 2015. High-resolution mass spectrometry and molecular characterization of aqueous photochemistry products of common types of secondary organic aerosols. J. Phys. Chem. A 119, 2594–2606. https://doi.org/10.1021/jp509476r.

Sarrafzadeh, M., Wildt, J., Pullinen, I., Springer, M., Kleist, E., Tillmann, R., Schmitt, S. H., Wu, C., Mentel, T.F., Zhao, D., Hastie, D.R., Kiendler-Scharr, A., 2016. Impact of NOx and OH on secondary organic aerosol formation from β-pinene photooxidation. Atmos. Chem. Phys. 16, 11237–11248. https://doi.org/10.5194/acp-16-11237-2016.

Shen, R.R., Liu, Z.R., Liu, Y.S., Wang, L.L., Li, D., Wang, Y.S., Wang, G.A., Bai, Y., Li, X.R., 2018. Typical polar organic aerosol tracers in $PM_{2.5}$ over the North China Plain: spatial distribution, seasonal variations, contribution and sources. Chemosphere 209, 758–766. https://doi.org/10.1016/j.chemosphere.2018.06.133.

Smith, J.D., Kinney, H., Anastasio, C., 2016. Phenolic carbonyls undergo rapid aqueous photodegradation to form low-volatility, light-absorbing products. Atmos. Environ. 126, 36–44. https://doi.org/10.1016/j.atmosenv.2015.11.035.

Smith, N.R., Montoya-Aguilera, J., Dabdub, D., Nizkorodov, S.A., 2021. Effect of humidity on the reactive uptake of ammonia and dimethylamine by nitrogen-containing secondary organic aerosol. Atmosphere 12, 1502. https://doi.org/10.3390/atmos12111502.

Volkamer, R., Ziemann, P.J., Molina, M.J., 2009. Secondary organic aerosol formation from acetylene (C_2H_2): seed effect on SOA yields due to organic photochemistry in the aerosol aqueous phase. Atmos. Chem. Phys. 9, 1907–1928. https://doi.org/10.5194/acp-9-1907-2009.

Wang, G., Zhang, R., Gomez, M.E., Yang, L., Levy Zamora, M., Hu, M., Lin, Y., Peng, J., Guo, S., Meng, J., Li, J., Cheng, C., Hu, T., Ren, Y., Wang, Y., Gao, J., Cao, J., An, Z., Zhou, W., Li, G., Wang, J., Tian, P., Marrero-Ortiz, W., Secrest, J., Du, Z., Zheng, J., Shang, D., Zeng, L., Shao, M., Wang, W., Huang, Y., Wang, Y., Zhu, Y., Li, Y., Hu, J., Pan, B., Cai, L., Cheng, Y., Ji, Y., Zhang, F., Rosenfeld, D., Liss, P.S., Duce, R.A., Kolb, C.E., Molina, M.J., 2016a. Persistent sulfate formation from London Fog to Chinese haze. Proc. Natl. Acad. Sci. U.S.A. 113, 13630–13635. https://doi.org/10.1073/pnas.1616540113.

Wang, Y.J., Luo, H., Jia, L., Ge, S.S., 2016b. Effect of particle water on ozone and secondary organic aerosol formation from benzene-NO_2-NaCl irradiations. Atmos. Environ. 140, 386–394. https://doi.org/10.1016/j.atmosenv.2016.06.022.

White J., S., Jamie M., I., Angove E., D., 2014. Chemical characterisation of semi-volatile and aerosol compounds from the photooxidation of toluene and NO_x. Atmos. Environ. 83, 237–244. https://doi.org/10.1016/j.atmosenv.2013.11.023.

Wildt, J., Mentel, T.F., Kiendler-Scharr, A., Hoffmann, T., Andres, S., Ehn, M., Kleist, E., Müsgen, P., Rohrer, F., Rudich, Y., Springer, M., Tillmann, R., Wahner, A., 2014. Suppression of new particle formation from monoterpene oxidation by NO_x. Atmos. Chem. Phys. 14, 2789–2804. https://doi.org/10.5194/acp-14-2789-2014.

Wu, C., Zhu, B., Liang, W., Ruan, T., Jiang, G., 2022. Molecular characterization of nitrogen-containing organic compounds in fractionated atmospheric humic-like substances (HULIS) and its relationship with optical properties. Sci. Total Environ. 832, 155043 https://doi.org/10.1016/j.scitotenv.2022.155043.

Xie, M., Chen, X., Hays, M.D., Lewandowski, M., Offenberg, J., Kleindienst, T.E., Holder, A.L., 2017. Light absorption of secondary organic aerosol: composition and contribution of nitroaromatic compounds. Environ. Sci. Technol. 51, 11607–11616. https://doi.org/10.1021/acs.est.7b03263.

Xu, L., Guo, H., Boyd, C.M., Klein, M., Bougiatioti, A., Cerully, K.M., Hite, J.R., Isaacman-VanWertz, G., Kreisberg, N.M., Knote, C., Olson, K., Koss, A., Goldstein, A.H., Hering, S.V., de Gouw, J., Baumann, K., Lee, S.H., Nenes, A., Weber, R.J., Ng, N.L., 2015. Effects of anthropogenic emissions on aerosol formation from isoprene and monoterpenes in the southeastern United States. Proc. Natl. Acad. Sci. U.S.A. 112, 37–42. https://doi.org/10.1073/pnas.1417609112.

Zhang, J., An, J., Qu, Y., Liu, X., Chen, Y., 2019a. Impacts of potential HONO sources on the concentrations of oxidants and secondary organic aerosols in the Beijing-Tianjin-Hebei region of China. Sci. Total Environ. 647, 836–852. https://doi.org/10.1016/j.scitotenv.2018.08.030.

Zhang, Q., Xu, Y., Jia, L., 2019b. Secondary organic aerosol formation from OH-initiated oxidation of *m*-xylene: effects of relative humidity on yield and chemical composition. Atmos. Chem. Phys. 19, 15007–15021. https://doi.org/10.5194/acp-19-15007-2019.

Zhang, R., Wang, G., Guo, S., Zamora, M.L., Ying, Q., Lin, Y., Wang, W., Hu, M., Wang, Y., 2015. Formation of urban fine particulate matter. Chem. Rev. 115, 3803–3855. https://doi.org/10.1021/acs.chemrev.5b00067.

Zhang, W.Y., Wang, W.G., Li, J.L., Peng, C., Li, K., Zhou, L., Shi, B., Chen, Y., Liu, M.Y., Ge, M.F., 2020. Effects of SO_2 on optical properties of secondary organic aerosol generated from photooxidation of toluene under different relative humidity conditions. Atmos. Chem. Phys. 20, 4477–4492. https://doi.org/10.5194/acp-20-4477-2020.

Zhang, Y.Z., Forrister, H., Liu, J.M., Dibb, J., Anderson, B., Schwarz, J.P., Perring, A.E., Jimenez, J.L., Campuzano-Jost, P., Wang, Y.H., Nenes, A., Weber, R.J., 2017. Top-of-atmosphere radiative forcing affected by brown carbon in the upper troposphere. Nat. Geosci. 10, 486–489. https://doi.org/10.1038/Ngeo2960.

Zhao, D., Schmitt, S.H., Wang, M., Acir, I.H., Tillmann, R., Tan, Z., Novelli, A., Fuchs, H., Pullinen, I., Wegener, R., Rohrer, F., Wildt, J., Kiendler-Scharr, A., Wahner, A., Mentel, T.F., 2018. Effects of NOx and SO_2 on the secondary organic aerosol formation from photooxidation of α-pinene and limonene. Atmos. Chem. Phys. 18, 1611–1628. https://doi.org/10.5194/acp-18-1611-2018.

Zou, Y., Deng, X.J., Zhu, D., Gong, D.C., Wang, H., Li, F., Tan, H.B., Deng, T., Mai, B.R., Liu, X.T., Wang, B.G., 2015. Characteristics of 1 year of observational data of VOCs, NO_x and O_3 at a suburban site in Guangzhou, China, Atmos. Chem. Phys. 15, 6625–6636. https://doi.org/10.5194/acp-15-6625-2015.